Int. J. Multiphase Flow Vol. 12, No. 2, pp. 169–184, 1986
Printed in Great Britain.

0301-9322/86 $3.00 + .00

STUDIES ON TWO-PHASE CROSS FLOW. PART II: TRANSITION REYNOLDS NUMBER AND DRAG COEFFICIENT

M. YOKOSAWA,† Y. KOZAWA, A. INOUE and S. AOKI
Research Laboratory for Nuclear Reactors, Tokyo Institute of Technology, Ohokayama, Meguro-ku, Tokyo, Japan

(*Received* 12 *June* 1984; *in revised form* 29 *March* 1985)

Abstract—A reduction of the transition Reynolds number from laminar separation to turbulent one of cross flow around a body is anticipated in a gas–liquid bubbly flow, since there exists intensive turbulence in the main flow. A decrease in the drag coefficient of the body can also be expected. This report was aimed to classify flow patterns of the two-phase wake flow behind a cylinder and to investigate quantitatively the change of the drag coefficient corresponding to the transition of the flow patterns. From measurements of the static pressure distribution on the cylinder surface and the drag coefficient of the cylinder, it was found that the flow pattern was sure to change finally into a new one similar to the transcritical type in the single-phase flow with an increase of the mean void fraction in the main flow. It was concluded that a large reduction of the upper transition Reynolds number occurred in a two-phase flow, because the transition could be realized by a little increase of the void fraction even below the lower transition Reynolds number in the case of a large cylinder diameter.

1. INTRODUCTION

It is very important for a plant to estimate pressure loss of flow in various conduits. A reduction of the pressure drop results in an improvement of the total plant efficiency. In many flow systems, complex conduits with flow obstacles have been widely employed and the flow in them is often gas–liquid two phase. Though hydraulic characteristics of cross flow around a obstacle, especially drag coefficient, are essential to estimate total pressure loss of such conduits, fundamental study on the two-phase cross flow has hardly been reported until now.

The single-phase cross flow around a cylinder is inevitably unsteady because of a periodic shedding of the Kármán vortices except for under the condition of the extremely low Reynolds number, i.e. $Re < 10^2$ (Pursnall & Loftin 1951; Delany & Sorensen 1953; Roshko 1954, 1955; Fung 1960; Roshko 1961). This wide range of Reynolds number is divided by the difference among the flow separation mechanisms into three regions which are commonly called subcritical, supercritical and transcritical, respectively. There exist the peculiar distributions of static pressure on the cylinder surface and the drag coefficient corresponding to each region, and these hardly change within each region. A Reynolds number between the subcritical region and the supercritical one is called the lower transition Reynolds number, more commonly the critical Reynolds number. A value between the supercritical region and the transcritical one is called the upper transition Reynolds number. In case of a cylinder, these values are reported as about 4×10^5 and 4×10^6, respectively. In these two transition Reynolds numbers, the lower critical Reynolds number is especially important for the engineering. When Reynolds number of the cross flow reaches the critical value, the drag coefficient decreases sharply from 1.2 to 0.3. Furthermore, when the Reynolds number exceeds the upper transition Reynolds number, the drag coefficient increases up to 0.8. Considering the transitions of the distribution of static pressure on the cylinder surface, the cause of changes of the drag coefficient have been explained to be in the fact that the separation mechanism in the boundary layer on the cylinder surface changes

†Present address: Nuclear & Process Engineering Department, Nuclear Project Division, JGC Co., Ohokubo, Kohonan-ku, Yokohama, Kanagawa, Japan.

from the laminar separation to the turbulent one, via the turbulent separation after the retouching behind the laminar separation point, as the Reynolds number increases. According as the separation mechanism changes, the separation angle goes initially back from 76° to about 130°, and then goes forward to the vicinity of 103°, which means that width of the wake region behind the cylinder narrows sharply and then recovers slightly. These changes of the drag coefficient and the transitions of the distribution of the static pressure with increasing of the Reynolds number are common in the case not only of cylinders but also all blunt bodies such as elliptic cylinders. The values of the drag coefficient, the separation angles and the two transition Reynolds numbers, however, depend not only on the shape of body but also the intensity of the turbulent velocity in the main flow (Surry 1972). When the intensity becomes large, the transition of the boundary layer from laminar to turbulent with an increase of the Reynolds number is promoted. Thus the critical Reynolds number decreases significantly.

In a gas–liquid bubbly flow, there exists more intensive turbulence, as compared with the single-phase flow, due to the disturbance induced by the bubbles. Moreover, since there appears large difference in the behaviors of both phases induced by the gradient of static pressure near the cylinder surface, the intensive turbulence is generated there. Momentum transported from the main flow to the boundary layer becomes fairly large in the two-phase flow. Therefore, large reduction in the transition Reynolds number seems to be realized in the two-phase cross flow. Consequently, total pressure loss of the two-phase flow can be reduced in such complex conduits with flow obstacles, as flow around rod spacers in a fuel assembly and flow across a cluster of pipes in a steam generator.

In this report, transition of flow patterns in the two-phase wake behind a cylinder were examined by measurement of the distribution of static pressure on the cylinder surface, and the change of the drag coefficient corresponding to the transition was correlated with the flow and geometrical conditions.

2. MEASURING PROCEDURES AND EXPERIMENTAL CONDITIONS

A hole with diameter 0.5 mm was drilled on the surface of the test cylinder to detect the static pressure on the cylinder surface. The distribution of the static pressure was measured by rotating the cylinder in θ-direction as shown in figure 1. The static pressure coefficient on the cylinder surface, i.e. Cp_{sur} could be obtained from the following equation:

$$Cp_{sur} = (p_{sur} - p_{\infty})/\Delta p_0, \qquad [1]$$

where p_{sur}, p_{∞} and Δp_0 were the static pressure on the cylinder surface, that in the case

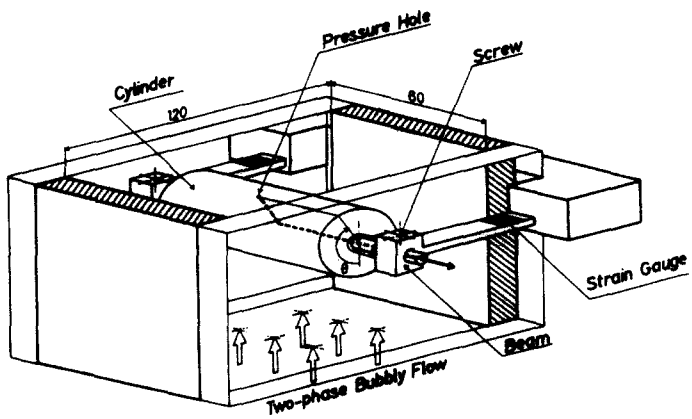

Figure 1. Test section for measurements of pressure distribution and drag coefficient.

without the test cylinder at the same measuring position and the dynamic pressure in the main flow, respectively.

When the drag coefficient Cd was measured, the cylinder was supported only by the two beams fixed at the one end. The center rods of the cylinder were anchored to the beams by screws to prevent the cylinder from rotating. From measuring the drag force D acting on the cylinder with the strain gauges mounted on the beam surfaces, Cd could be obtained as follows:

$$Cd = D/(\Delta p_0 \cdot d \cdot l), \qquad [2]$$

where d and l were the diameter and the length of the test cylinder.

The result of Cd was always equal to the value obtained by integrating the static pressure on the cylinder surface, within errors ±4%.

The other measuring procedures were mentioned in our first report.

The experimental conditions in this report are tabulated as follows:

Dimension of the two-phase flow duct		120 × 60 mm
Diameter of the test cylinder	d	1, 3, 5, 6, 8, 10, 20, 30 and 40 mm
Diameter of bubbles		3 ~ 5 mm
Mean diameter of bubbles	d_b	about 4 mm
Mean void fraction in the main flow	$\bar{\alpha}_0$	0–0.1
Mean velocity in the main flow	$\bar{U}_{0.TP}$	1–5 m/s
Reynolds number of the two-phase flow	Re_{TP}	4×10^3–3×10^5

$\bar{U}_{0.TP}$ and Re_{TP} were calculated as the following equations.

$$\bar{U}_{0.TP} = \{2\Delta p_0/[\rho_L(1 - \bar{\alpha}_0) + \rho_G\bar{\alpha}_0]\}^{1/2} \qquad [3]$$

$$\mathrm{Re}_{TP} = \bar{U}_{0.TP}d/\nu_L, \qquad [4]$$

where ρ_L and ρ_G were the density of liquid- and gas-phase, respectively. In [4], the dynamic viscosity of liquid ν_L was used in the definition of Re_{TP} because the liquid layer which was several times as thick as the boundary layer always veiled the whole of cylinder surface.

3. EXPERIMENTAL RESULTS

3.1 *Distribution of static pressure on the cylinder surface*

The cylinder diameters larger than 10 mm, i.e. 10, 20, 30 and 40 mm, were used in the measurements of the distribution of static pressure on the cylinder surface. Similar distributions appeared throughout the Re_{SP} range in the case of $d = 10$ mm, since the range of the Reynolds number of the liquid single-phase flow, i.e. $0.13 \times 10^5 \leq \mathrm{Re}_{SP} \leq 0.63 \times 10^5$, was in the subcritical region. On the other hand, in case of $d = 40$ mm, the distribution changed from the subcritical type to the supercritical one at near $\mathrm{Re}_{SP} = 1 \times 10^5$, because the range in this case, i.e. $0.5 \times 10^5 \leq \mathrm{Re}_{SP} \leq 3 \times 10^5$, involved the critical Reynolds number. The reason of a reduction in the critical Reynolds number into one-fourth of the ordinary value is considered to be mainly the influence of the turbulence in the main flow (Surry 1972).

Effect of the cylinder diameter d is shown in figure 2, where $\bar{\alpha}_0$ are the same and Re_{TP} is fixed at the subcritical value in the single-phase flow. As the references three curves of the single-phase flow are also shown, where two of them at $\mathrm{Re}_{SP} = 0.5 \times 10^5$ are the typical of the subcritical type *Sub* and the other at $\mathrm{Re}_{TP} = 2.5 \times 10^5$ is the typical of the supercritical one *Sup*. The large difference in the static pressure in the backward region of the cylinder

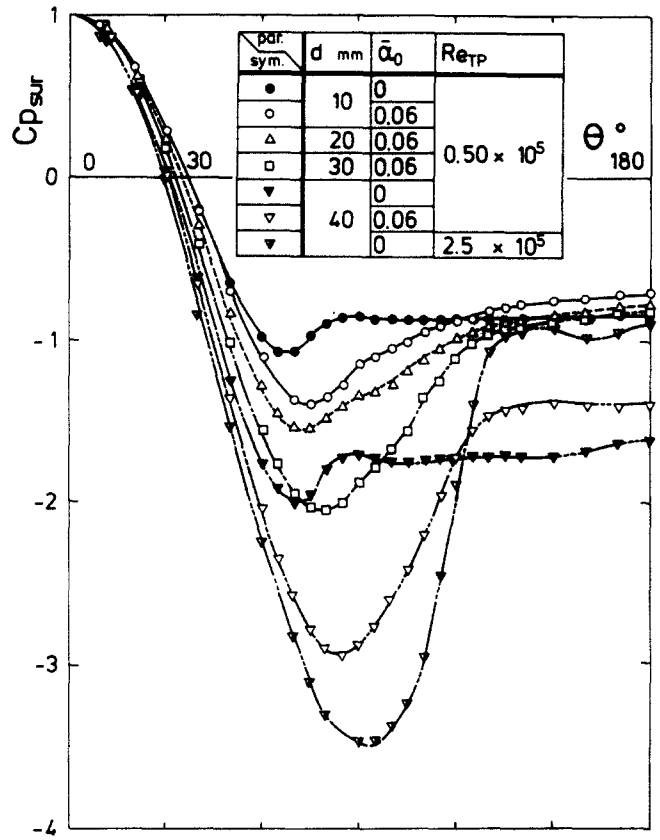

Figure 2. Effect of cylinder diameter d on distribution of static pressure on cylinder surface ($\bar{\alpha}_0$ = 0.06, $Re_{TP} = 0.50 \times 10^5$).

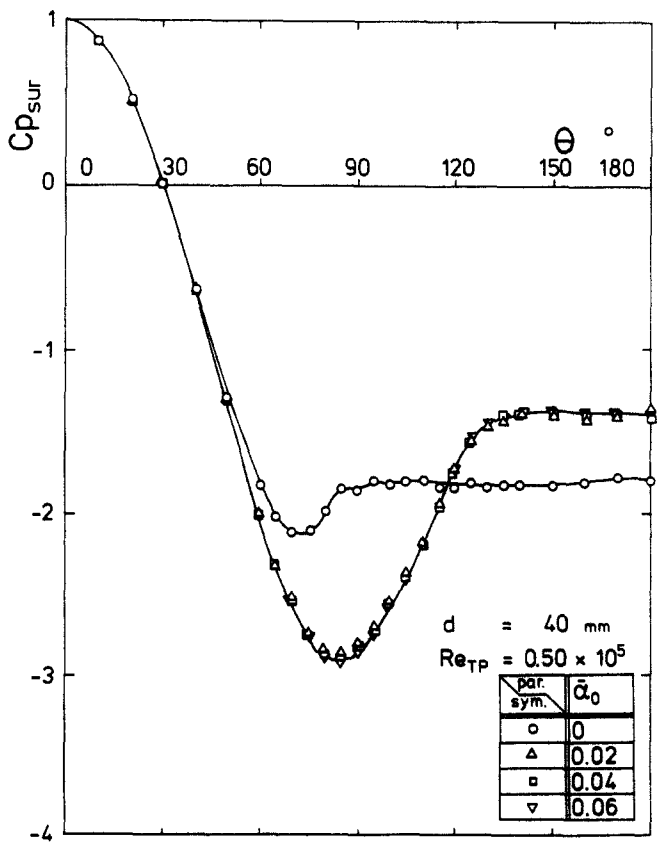

Figure 3. Effect of mean void fraction in main flow $\bar{\alpha}_0$ on distribution of static pressure on cylinder surface (d = 40 mm, $Re_{TP} = 0.50 \times 10^5$).

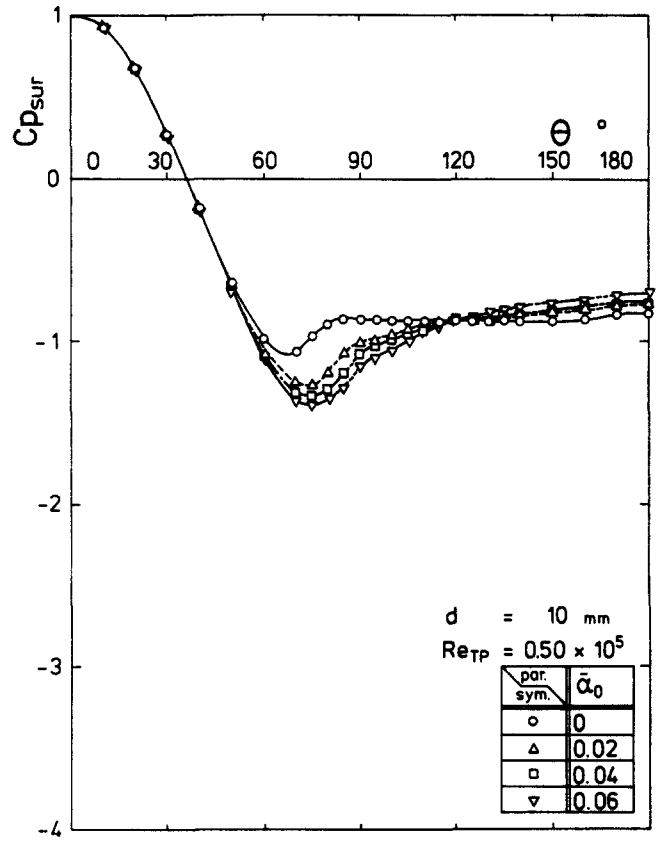

Figure 4. Effect of mean void fraction in main flow $\bar{\alpha}_0$ on distribution of static pressure on cylinder surface (d = 10 mm, Re_{TP} = 0.50 × 10^5).

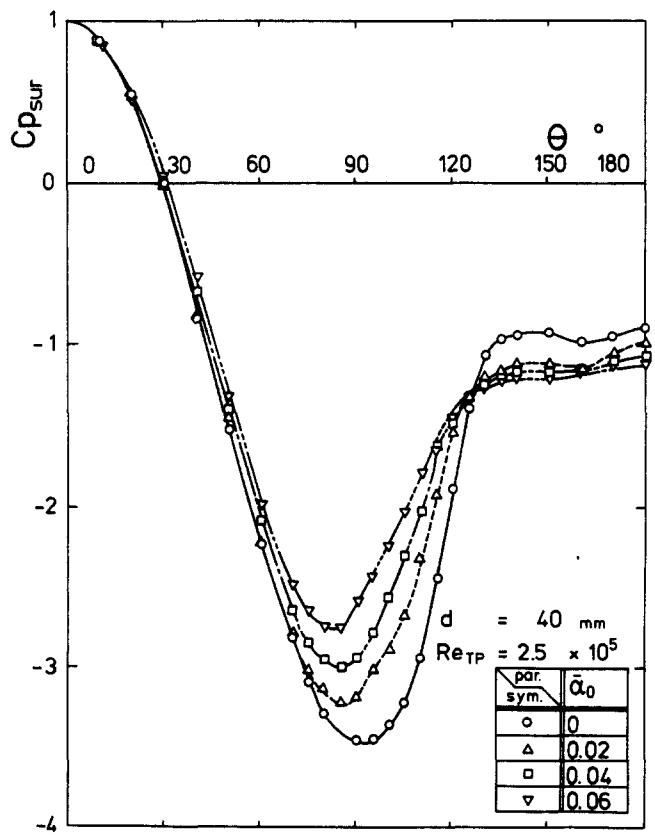

Figure 5. Effect of mean void fraction in main flow $\bar{\alpha}_0$ on distribution of static pressure on cylinder surface (d = 40 mm, Re_{TP} = 2.5 × 10^5).

between $d = 10$ and 40 mm at $Re_{SP} = 0.5 \times 10^5$ in the single-phase flow is caused by a ratio of the cylinder diameter d to width of the duct h, namely the blockage d/h.

In case of $d = 10$ mm, though the distribution in the two-phase flow was similar to that of *Sub* in the single-phase flow, minimum pressure got somewhat low, the separation point shifted backward slightly and the pressure in back of the separation point recovered gently. On the other hand, in case of $d = 40$ mm, a new type *TPTrans* of the distribution which clearly differed from both *Sub* and *Sup* in the single-phase flow appeared. The new type has a neutral shape between these two types in the single-phase flow. This is suggestive of the transcritical type *Trans* in the single-phase flow and we call the two-phase transcritical type *TPTrans*.

The dependency on the mean void fraction $\bar{\alpha}_0$ at $Re_{TP} = 0.5 \times 10^5$ in case of $d = 40$ mm is shown in figure 3. The transition was almost terminated at $\bar{\alpha}_0 = 0.02$, and almost similar distribution was kept for further increment of $\bar{\alpha}_0$. In the case of $d = 10$ mm, there was little advance in the transition by the condition up to $\bar{\alpha}_0 = 0.06$ as shown in figure 4. Considering together that the transition occurred gradually with respect to d as shown in figure 2, the transition from the subcritical type *Sub* to the new one *TPTrans* with increasing of $\bar{\alpha}_0$ appeared at any d. Moreover, $\bar{\alpha}_0$ where the transition terminated moved to lower value with increasing of d. The distribution at $Re_{TP} = 2.5 \times 10^5$ in the case of $d = 40$ mm is shown in figure 5 for various $\bar{\alpha}_0$. The distribution under this condition changed from the supercritical type *Sup* to the new one *TPTrans* with increasing of $\bar{\alpha}_0$. As compared with the case at $Re_{TP} = 0.5 \times 10^5$, the distribution changes gradually with $\bar{\alpha}_0$ and the transition seems not to be terminated yet at $\bar{\alpha}_0 = 0.06$. It is finally concluded that the distribution of Cp_{sur} changed finally to *TPTrans* with increasing of the mean void fraction in the two-phase flow from *Sub* for low and *Sup* for high Reynolds number in the single-phase flow.

The dependency of the distribution on the Reynolds number Re_{TP} is shown in figures 6, 7 and 8 in which cylinder diameters are different from one another. In the case of $d = 10$ mm, as Re_{TP} is limited sufficiently below the critical Reynolds number in the single-phase flow, the distribution does not depend on Re_{TP} as shown in figure 6. Also in the case of $d = 20$ mm shown in figure 7, there is little dependency under the condition of $Re_{TP} \leq 0.5 \times 10^5$. However, the transition corresponding to the lower transition in the single-phase flow is recognized under the condition of $Re_{TP} \geq 0.75 \times 10^5$. In case of $d = 40$ mm shown in figure 8, the distribution hardly depends on Re_{TP} and shifts to *TPTrans*, though the critical Reynolds number is included in the region of the experimental condition of Re_{TP}. This result suggests that the abovementioned transition from *Sub* or *Sup* in the single-phase flow to *TPTrans* in the two-phase flow with increment of $\bar{\alpha}_0$ has almost terminated at $\bar{\alpha}_0 = 0.06$.

3.2 *Drag coefficient of a cylinder*

The experimental results of the drag coefficient in cases of $d = 40$ and 20 mm are shown in figures 9 and 10, respectively. A ratio of the drag coefficient in the two-phase flow Cd_{TP} to that in the subcritical region of the liquid single-phase flow $(Cd_{SP})_{Sub}$ was investigated to eliminate as far as possible the effects of a ratio of the cylinder diameter d to the width of the duct h, the so-called blockage d/h, and a ratio of the cylinder length l to the cylinder diameter d, l/d. If contributions of d/h and l/d to the drag coefficient in the two-phase flow are the same as those in the single-phase flow, the effects of these two parameters may be completely eliminated by taking the ratio of both drag coefficients.

When Re_{TP} was sufficiently lower than the critical Reynolds number of the single-phase flow, i.e. $Re_{TP} \leq 0.63 \times 10^5$, $Cd_{TP}/(Cd_{SP})_{Sub}$ decreased with increase of $\bar{\alpha}_0$ and were independent of the mean velocity in the main flow $\bar{U}_{0.TP}$. The larger d became, the more significant the trend of this reduction in the drag coefficient got. $Cd_{TP}/(Cd_{SP})_{Sub}$, especially in the case of $d = 40$ mm, approached rapidly to 0.6 as $\bar{\alpha}_0$ increased from 0 to about 0.01, and then kept the constant value. This change of the drag coefficient with increasing of $\bar{\alpha}_0$

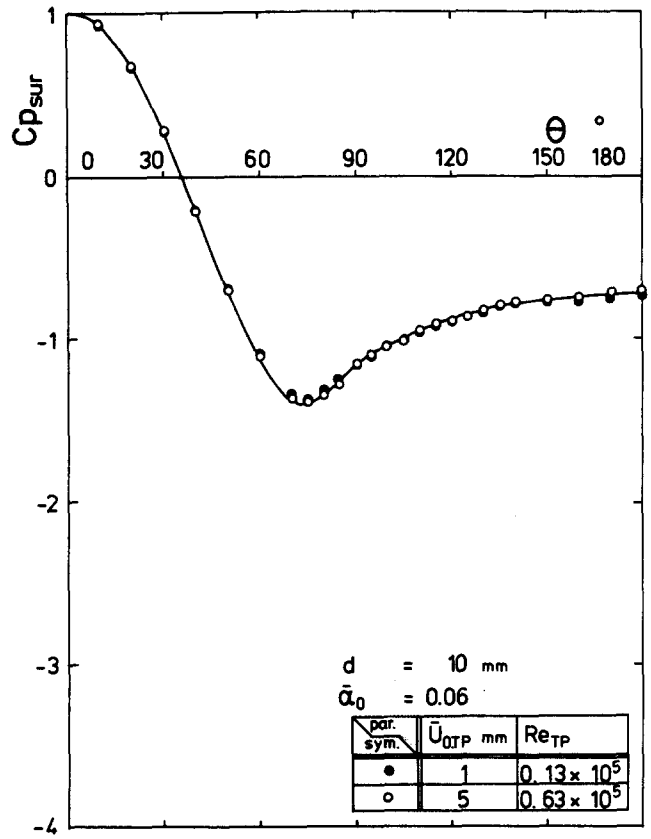

Figure 6. Effect of Reynolds number of two-phase flow Re_{TP} on distribution of static pressure on cylinder surface (d = 10 mm, $\bar{\alpha}_0$ = 0.06).

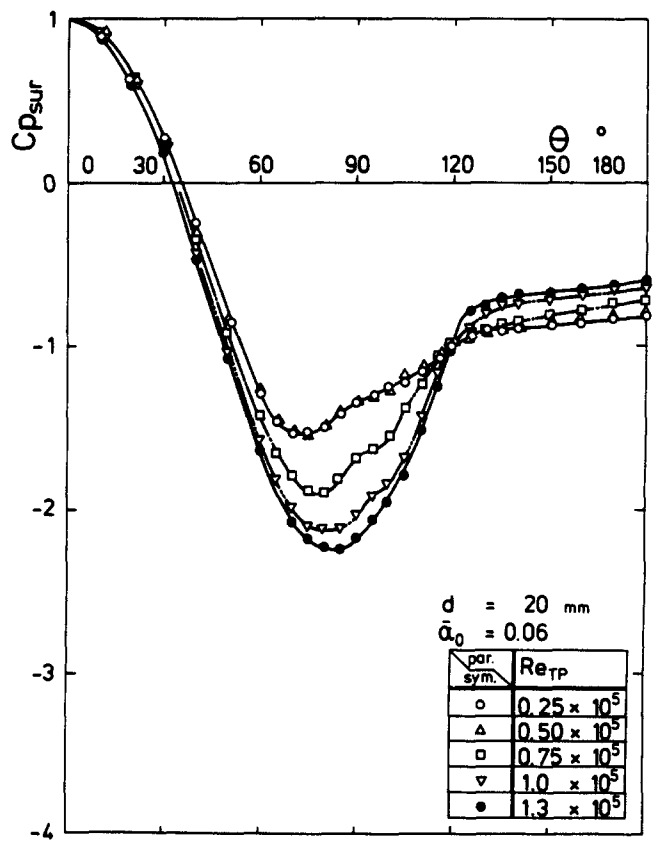

Figure 7. Effect of Reynolds number of two-phase flow Re_{TP} on distribution of static pressure on cylinder surface (d = 20 mm, $\bar{\alpha}_0$ = 0.06).

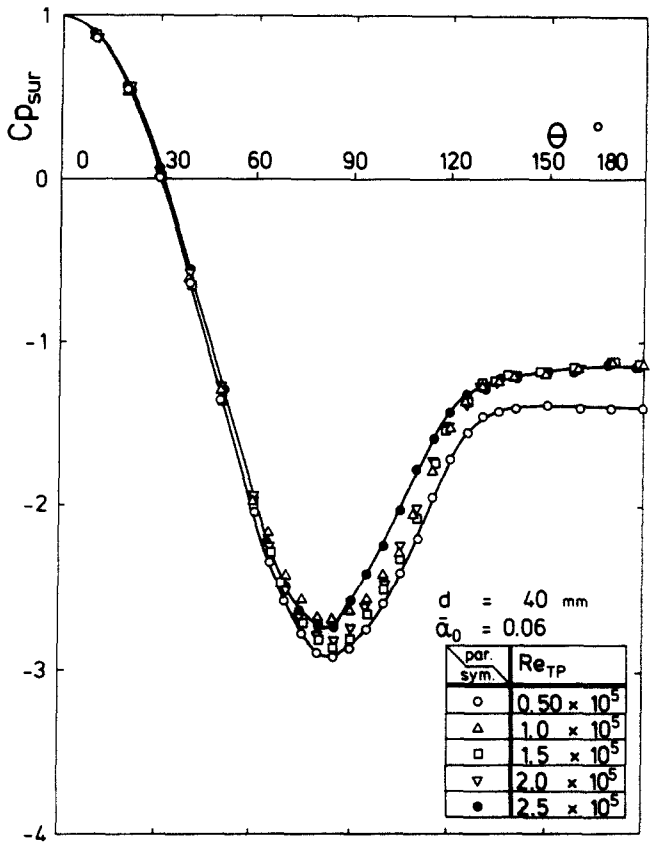

Figure 8. Effect of Reynolds number of two-phase flow Re_{TP} on distribution of static pressure on cylinder surface (d = 40 mm, $\bar{\alpha}_0$ = 0.06).

corresponds to the abovementioned transition from the subcritical type *Sub* in the single-phase flow to the new one *TPTrans* in the two-phase flow, so that

$$(Cd_{TP})_{TPTrans}/(Cd_{SP})_{Sub} = 0.60 \quad [5]$$

On the other hand, when Re_{TP} was larger than the critical Reynolds number, $Cd_{TP}/(Cd_{SP})_{Sub}$ increased smoothly from the value about 0.40 of the supercritical type *Sup* in the single-phase flow to that about 0.6 of *TPTrans* with increase of $\bar{\alpha}_0$, which is corresponding to the transition of the distribution of Cp_{sur} from the supercritical type *Sup* in the single-phase flow to *TPTrans*. The drag coefficient was almost independent of $\bar{U}_{0.TP}$ as well as d after the transition.

When Re_{TP} was about the critical Reynolds number, $Cd_{TP}/(Cd_{SP})_{Sub}$ decreased from a value between those of *Sub* and *Sup* to about 0.6 of *TPTrans*.

The result in the cases of $d \leq 10$ mm under condition of $Re_{TP} \leq 0.63 \times 10^5$ was shown in figure 11 in the lump. The drag coefficients for d = 10 and 6 mm were almost equal and decreased a little with increasing of $\bar{\alpha}_0$. For d = 10 mm, as shown in figure 4, there was no large difference between the distribution of Cp_{sur} in the two-phase flow and that of the subcritical type *Sub* in the single-phase flow. Therefore, it was considered that the wake flow was always similar to that of *Sub* under the $\bar{\alpha}_0$ condition where the drag coefficient decreased gradually with increasing of $\bar{\alpha}_0$.

In cases of $d < 6$ mm, the reduction in the drag coefficient with increase of $\bar{\alpha}_0$ appeared in low $\bar{\alpha}_0$ conditions and more remarkable than that in cases of d = 10 and 6 mm. The smaller the cylinder diameter d became, the larger the reduction appeared. In these small cylinder experiments, it was observed, several bubbles were trapped into the wake region behind the cylinder and they clung on the back surface of the cylinder. These bubbles were soon stripped by the Kármán vortices and shed to the downstream. The number of bubbles in the wake

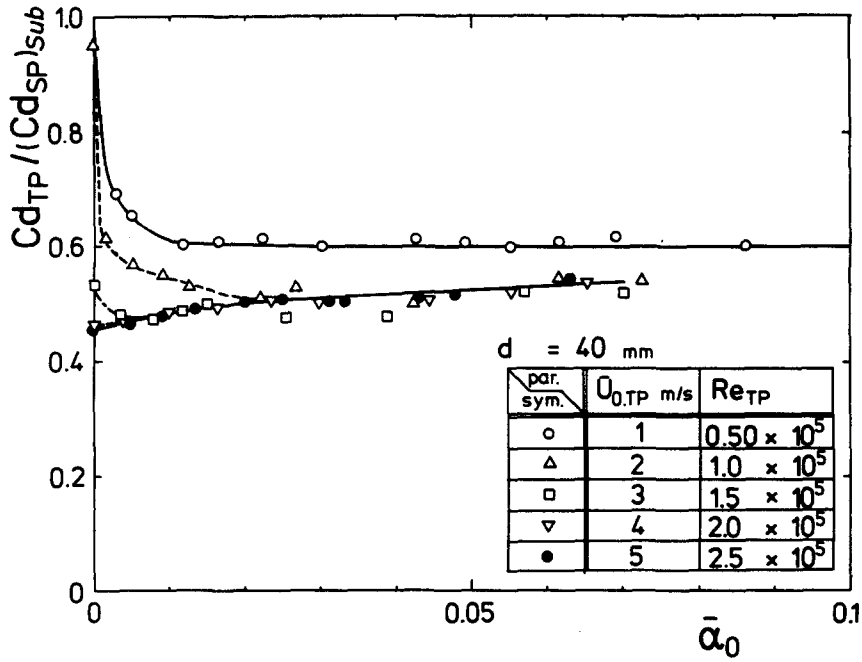

Figure 9. Drag coefficient ratio $Cd_{TP}/(Cd_{SP})_{Sub}$ against mean void fraction in main flow $\bar{\alpha}_0$ (d = 40 mm).

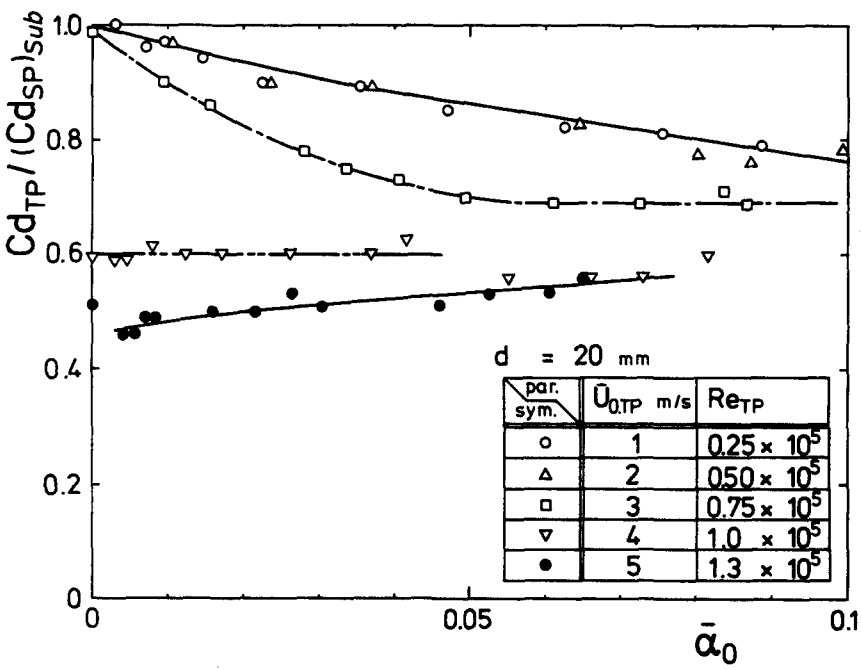

Figure 10. Drag coefficient ratio $Cd_{TP}/(Cd_{SP})_{Sub}$ against mean void fraction in main flow $\bar{\alpha}_0$ (d = 20 mm).

region was kept almost constant as illustrated in figure 12.1. As $\bar{\alpha}_0$ increased, the number of the clinging bubbles also increased (figure 12.2). Coalescence of these bubbles hardly occurred in low $\bar{\alpha}_0$ conditions. When $\bar{\alpha}_0$ increased up to a certain critical value, the bubbles covered over the all portion in direction of the cylinder axis to fill the back surface of the cylinder [figure 12.3(a)], coalesced rapidly [figure 12.3(b)], and then formed a cavity [figure 12.3(c), (d)]. Finally the cavity developed into the stable one [figure 12.3(e)] absorbing the bubbles of the main flow from both sides of the cavity, i.e. the transition to the cavity flow *Cav* took place. On the other hand, when $\bar{\alpha}_0$ decreased, the cavity flow

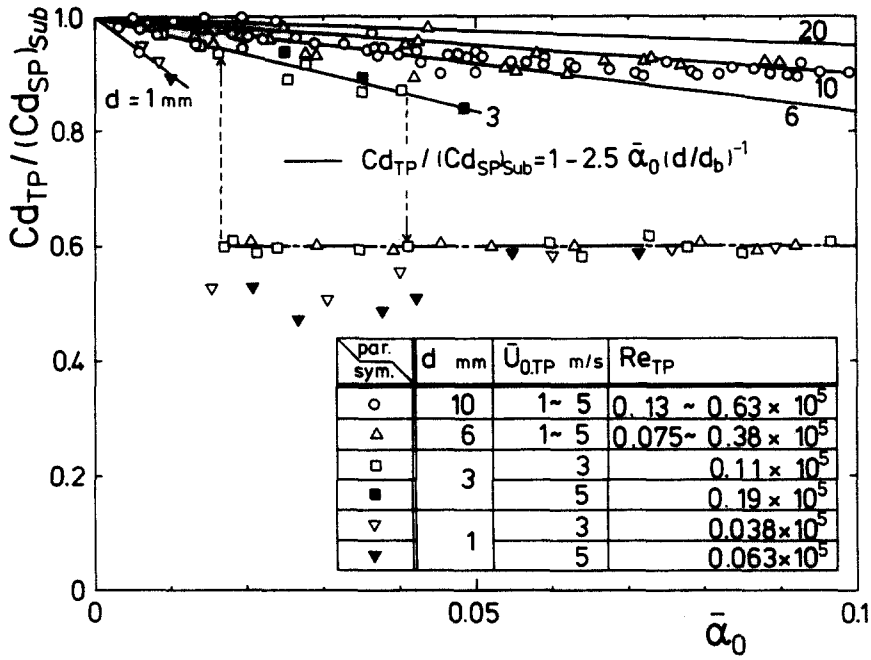

Figure 11. Drag coefficient ratio $Cd_{TP}/(Cd_{SP})_{Sub}$ against mean void fraction in main flow $\bar{\alpha}_0$ ($d < 10$ mm).

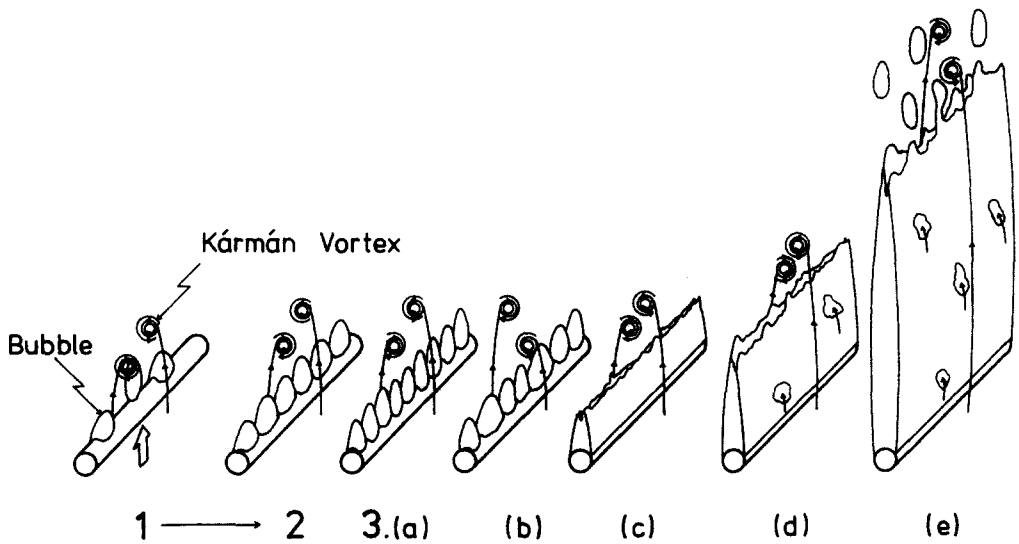

Figure 12. Transition process from subcritical type to cavity flow.

disappeared and the flow around the cylinder was restored again to the former state. However, the *Cav* → *Sub* transition occurred at lower value of $\bar{\alpha}_0$ than that of the *Sub* → *Cav* transition, i.e. there existed a hysteresis of the transitions. The transitions were easily detected by the observation as well as the measurements of the drag coefficient as shown in figures 13 and 14. The broken lines in figure 11 show the transitions under the condition of $d = 3$ mm and $\bar{U}_{0.TP} = 3$ m/s. $\bar{\alpha}_0$ at the *Sub* → *Cav* transition increased with $\bar{U}_{0.TP}$. Under the condition of $\bar{U}_{0.TP} \leq 1$ m/s, the *Sub* → *Cav* transition never appeared since the buoyant force acting on bubbles prevented them from clinging on the back surface. As d decreased, the number of the bubbles stripped by the Kármán vortices sharply decreased, because the scale of the Kármán vortex became equal to or smaller than the mean bubble diameter d_b. Consequently, the *Sub* → *Cav* transition took place at a smaller $\bar{\alpha}_0$ as shown in figure 13.

In cases of $d \geq 6$ mm, the cavity flow was formed for a time by attaching of the

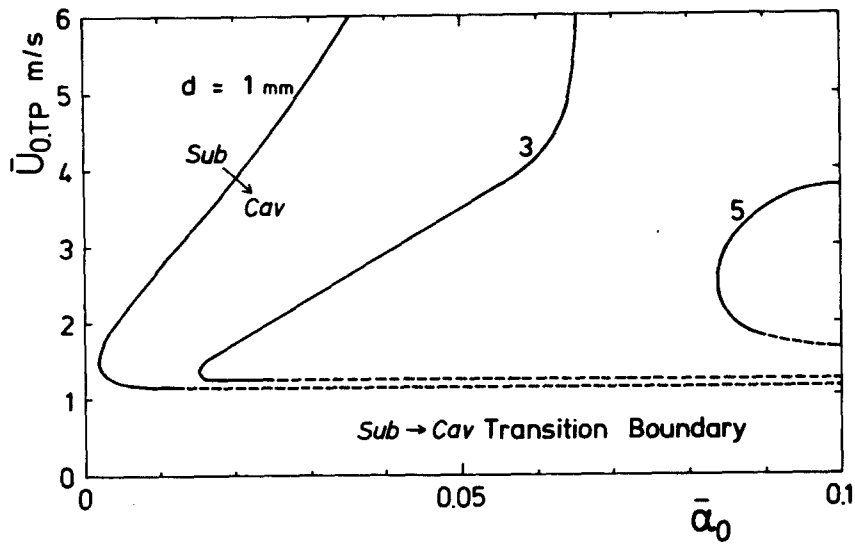

Figure 13. Transition boundary from subcritical type *Sub* to cavity flow *Cav*.

comparatively large bubbles about 10 mm, but the cavity flow was stable only within the narrow region near $\bar{U}_{0.TP} = 3$ m/s as clearly shown by the *Cav* → *Sub* transition boundary in the case of $d = 8$ mm in figure 14.

When $\bar{U}_{0.TP}$ increased further from a condition under which the cavity flow appeared as shown in figure 12.3(e), the separation of bubbles from the rear end of the cavity was activated. When $\bar{\alpha}_0$ decreased, the number of the bubbles absorbed from both sides of the cavity decreased. The cavity, therefore, got gradually shorter. When $\bar{\alpha}_0$ decreased further, the whole cavity was stripped off at a certain value of $\bar{\alpha}_0$ to change suddenly from the state in figure 12.3(e) to that in figure 12.2.

Photographs of two kinds of flow patterns under a condition of the hysteresis region are shown in figure 15. Bubbles in the wake were absorbed from both sides of the cavity. The rear end of the cavity was unstable and disintegrated into bubbles again there. The ratio of the cavity width to the cylinder diameter, w/d, was about 2.5 almost independent of d, $\bar{\alpha}_0$ and Re_{TP}. The cavity length was scores of times as large as d and seemed to shorten with decrease of d, although the rear end of the cavity was indistinct. The drag coefficient ratio of the cavity flow $(Cd_{TP})_{Cav}/(Cd_{SP})_{Sub}$ was independent of $\bar{\alpha}_0$ and Re_{TP} except for the slightly low

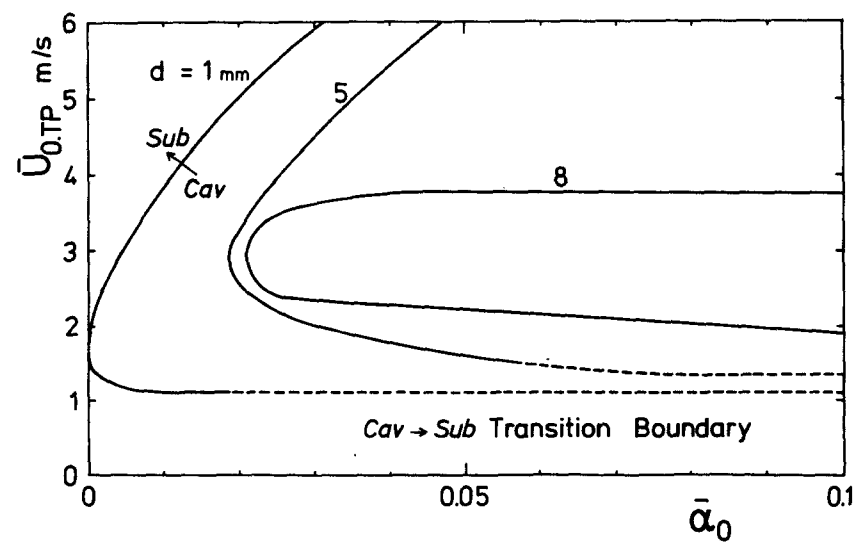

Figure 14. Transition boundary from cavity flow *Cav* to subcritical type *Sub*.

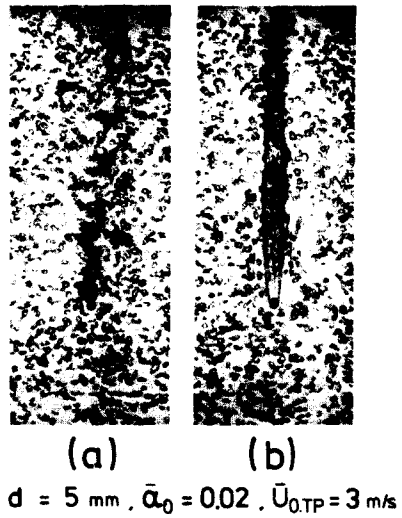

Figure 15. Photographs of two kinds of flow patterns, subcritical type (a) and cavity flow (b), under condition of histerisis region.

value under the condition of $d = 1$ mm and $\bar{\alpha}_0 \leq 0.05$ as shown in figure 11. The ratio could be correlated as

$$(Cd_{TP})_{Cav}/(Cd_{SP})_{Sub} = 0.60. \quad [6]$$

4. DISCUSSIONS

4.1 *Transition Reynolds number in the two-phase flow*

From the experiments of the static pressure on the cylinder surface, it was found that the static pressure distribution in the two-phase flow changed from the subcritical type *Sub* or the supercritical one *Sup* in the single-phase flow to the new one *TPTrans* observed in the two-phase flow with increasing of $\bar{\alpha}_0$. This new type was similar to the transcritical type *Trans* in the single-phase flow. The pressure distribution of *TPTrans* had a neutral shape between *Sub* and *Sup* in the single-phase flow. Assuming that the separation angle θ_{sep} is the location where the static pressure on the cylinder surface recovers up to the back pressure, the value was obtained from the distribution of the static pressure as shown in figure 16.

In case of $d = 10$ mm, the separation angle θ_{sep} only slightly increases from 80° to 90° as $\bar{\alpha}_0$ increases. This result suggests that the transition from *Sub* to *TPTrans* hardly occurs as already shown in figure 4.

On the other hand, in the case of $d = 40$ mm under the condition of $Re_{TP} \leq 0.63 \times 10^5$, θ_{sep} rapidly goes back from 80° to 120° as $\bar{\alpha}_0$ increases by about 0.005. This shows the sharp transition from *Sub* to *TPTrans*. Under the condition of $Re_{TP} \geq 1.3 \times 10^5$, θ_{sep} goes ahead from 130° to 120° with increasing of $\bar{\alpha}_0$. Under the condition of $0.63 \times 10^5 < Re_{TP} < 1.3 \times 10^5$, θ_{sep} changes from the moderate value between 120° and 130° to reach the curve under the condition of $Re_{TP} \geq 1.3 \times 10^5$.

As mentioned in section 1, the drag coefficient ratio of the transcritical type to the subcritical one, $(Cd_{SP})_{Trans}/(Cd_{SP})_{Sub}$, is about 0.67 and θ_{sep} is 103°. That of *TPTrans* $(Cd_{TP})_{TPTrans}/(Cd_{SP})_{Sub}$ was 0.6 and θ_{sep} was 120°. Thus, the drag coefficients of *Trans* in the single-phase flow and *TPTrans* in the two-phase flow are nearly the same value and both separation angles exist ahead of that of *Sup* in the single-phase flow. If the new type *TPTrans* in the two-phase flow is the transcritical one in the two-phase flow, the significant dip in the transition Reynolds number as mentioned in section 1 is realized. Furthermore, considering that this transition with increasing of $\bar{\alpha}_0$ appears even under the condition of $Re_{TP} \leq 0.63 \times 10^5$, it seems to be that the upper transition Reynolds number in the two-phase flow declines below the critical Reynolds number in the single-phase flow.

Under these conditions, the distribution of static pressure changed almost into the

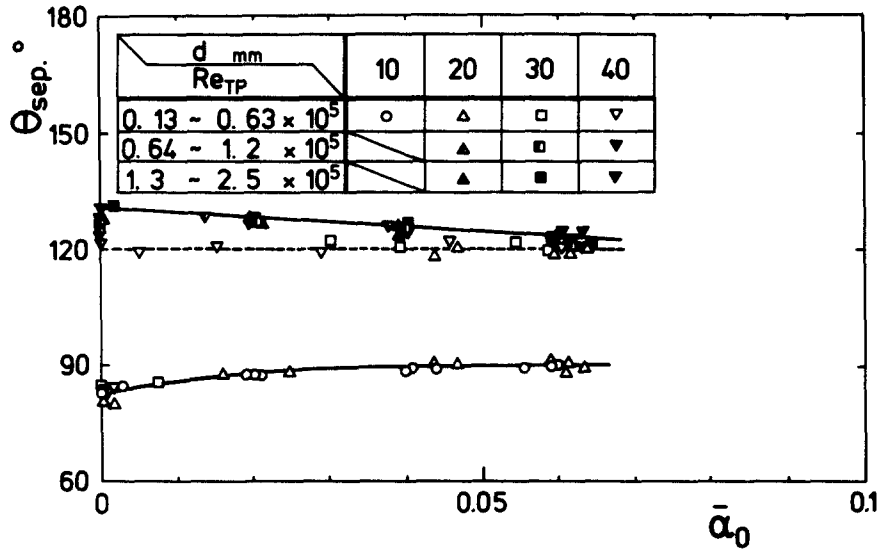

Figure 16. Effects of cylinder diameter d and mean void fraction in main flow $\bar{\alpha}_0$ on separation angle θ_{sep}.

transcritical type in the two-phase flow *TPTrans*, at any Re_{TP} with increasing of $\bar{\alpha}_0$, in the cases of $d \geq 20$ mm. Especially, under conditions of $d \geq 30$ mm and $Re_{TP} \leq 0.63 \times 10^5$, since the change of the drag coefficient was comparatively large, the value of $\bar{\alpha}_0$ at which the transition terminated could be obtained from the point where $Cd_{TP}/(Cd_{SP})_{Sub}$ decreased to 0.6 as shown in figure 9. Figure 17 shows the boundary value of $\bar{\alpha}_0$ corresponding to the upper transition Reynolds number in the two-phase flow. As the cylinder diameter becomes large, the value becomes small, i.e. the region of *TPTrans* enlarges.

4.2 *Experimental formulas of the drag coefficient*

As mentioned in the section 3.2, in cases of $d \geq 20$ mm, the drag coefficient ratio $Cd_{TP}/(Cd_{SP})_{Sub}$ was independent of $\bar{U}_{0.TP}$ under the condition of $Re_{TP} \leq 0.63 \times 10^5$, and of Re_{TP} under the condition of $Re_{TP} \geq 1.3 \times 10^5$. $Cd_{TP}/(Cd_{SP})_{Sub}$ in these two regions were separately arranged as shown in figures 18 and 19. In cases of $d \geq 20$ mm under the condition of $Re_{TP} \leq 0.63 \times 10^5$, $Cd_{TP}/(Cd_{SP})_{Sub}$ was sharply decreased from 1 to 0.6 as $\bar{\alpha}_0$ increased, where the values of 1 and 0.6 corresponded to *Sub* in the single-phase flow and *TPTrans* in the two-phase flow, respectively. These experimental data could be correlated by the following empirical formula within errors ±5%.

$$Cd_{TP}/(Cd_{SP})_{Sub} = 0.60 + 0.40 \,\mathrm{Exp}\,[-\bar{\alpha}_0(8.67d/h)^6]$$

$$20 \text{ mm} \leq d \leq 40 \text{ mm},\ 0 \leq \bar{\alpha}_0 \leq 0.1,\ 0.19 \times 10^5 \leq Re_{TP} \leq 0.63 \times 10^5;\quad h = 120 \text{ mm}, \quad [7]$$

where d/h means the flow blockage. This formula may be expressed by l/d or d/d_b, instead of d/h. However, the effect of l/d is small in the duct with the depth equal to the cylinder length. Suggesting that the tiny hydrogen bubbles used at measurements of velocity profiles in various water flows have hardly effect on the flow, the effect of d/d_b must weaken when it becomes large. The correlation by l/d or d/d_b are, therefore, unreasonable.

On the other hand, under the condition of $Re_{TP} \geq 1.3 \times 10^5$, $Cd_{TP}/(Cd_{SP})_{Sub}$ increased gradually with $\bar{\alpha}_0$ and finally reached 0.6 corresponding to *TPTrans*. However, $Cd_{TP}/(Cd_{SP})_{Sub}$ continued to increase in the region of this experimental conditions because the influence of $\bar{\alpha}_0$ was weak. In this case, $Cd_{TP}/(Cd_{SP})_{Sub}$ could be correlated within errors ±8% as follows:

$$Cd_{TP}/(Cd_{SP})_{Sub} = 0.46 + 0.64\,\bar{\alpha}_0^{3/4}$$

$$20 \text{ mm} \leq d \leq 40 \text{ mm},\ 0 \leq \bar{\alpha}_0 \leq 0.1,\ 1.3 \times 10^5 \leq Re_{TP} \leq 2.5 \times 10^5 \quad [8]$$

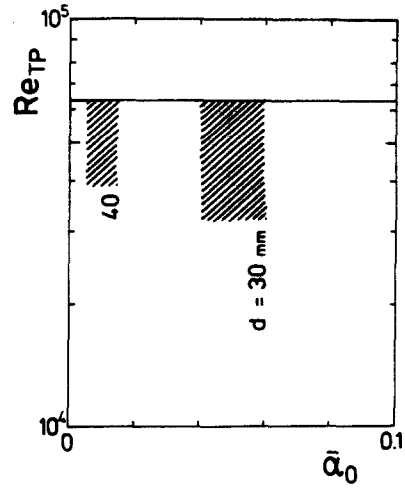

Figure 17. Boundary value of mean void fraction in main flow $\bar{\alpha}_0$ corresponding to upper transition Reynolds number in two-phase flow.

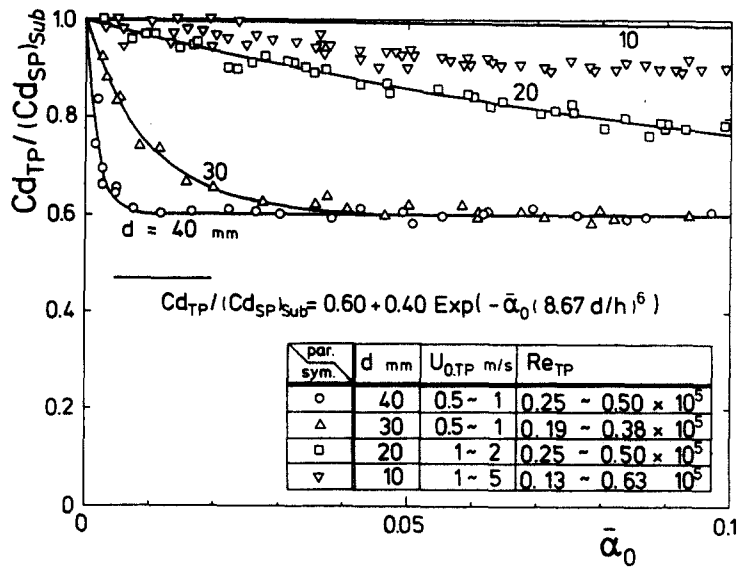

Figure 18. Drag coefficient ratio $Cd_{TP}/(Cd_{SP})_{Sub}$ against mean void fraction in main flow $\bar{\alpha}_0$ ($0.13 \times 10^5 \leq Re_{TP} \leq 0.63 \times 10^5$).

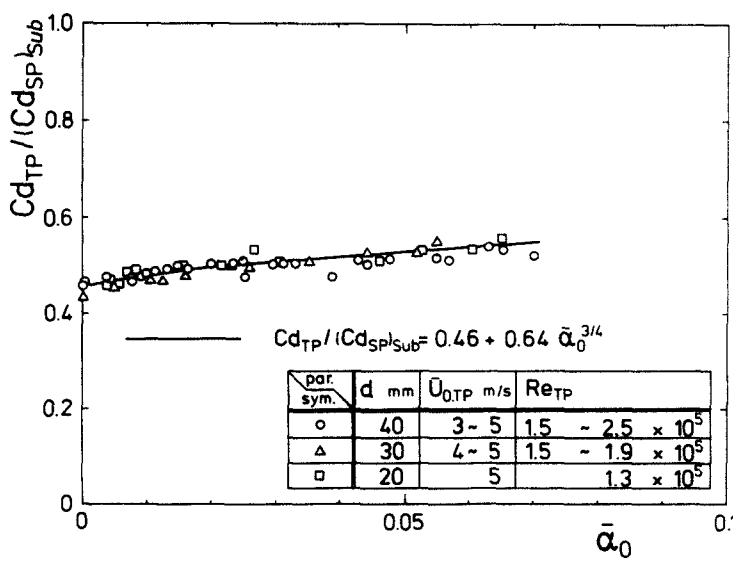

Figure 19. Drag coefficient ratio $Cd_{TP}/(Cd_{SP})_{Sub}$ against mean void fraction in main flow $\bar{\alpha}_0$ ($1.3 \times 10^5 \leq Re_{TP} \leq 2.5 \times 10^5$).

As shown in figure 18, in cases of $d \leq 10$ mm, the formula [7] was not fit. In these cases, bubbles clung on the back surface of the cylinder. These bubbles can be regarded as partial cavities formed along the axis of the cylinder. The number of the bubbles increased with increasing of $\bar{\alpha}_0$, which brought about the reduction in $Cd_{TP}/(Cd_{SP})_{Sub}$ in figure 11. Effects of d/h and l/d are negligible in these cases. Consequently, assuming that the number of the bubbles clinging on the back surface of the cylinder was ruled by d/d_b, the experimental data could be correlated as the following formula within errors ±7%.

$$Cd_{TP}/(Cd_{SP})_{Sub} = 1 - 2.5 \cdot \bar{\alpha}_0 (d/d_b)^{-1}$$

$$1\text{mm} \leq d \leq 10 \text{ mm}, 0 \leq \bar{\alpha}_0 \leq 0.1, 0.038 \times 10^5 \leq \text{Re}_{TP} \leq 0.63 \times 10^5 \quad [9]$$

Here, as shown in figures 11 and 18, the formulas [7] and [9] are almost unity in the cases of $d \leq 10$ mm and $d \geq 20$ mm, respectively. Therefore, multiplying the two formulas, the formula which covers all diameters in this experiments can be obtained as follows:

$$Cd_{TP}/(Cd_{SP})_{Sub} = \{0.60 + 0.40 \text{ Exp } [-\bar{\alpha}_0 (8.67\, d/h)^6]\} [1 - 2.5 \cdot \bar{\alpha}_0 (d/d_b)^{-1}]$$

$$1 \text{ mm} \leq d \leq 40 \text{ mm}, 0 \leq \bar{\alpha}_0 \leq 0.1, 0.038 \times 10^5 \leq \text{Re}_{TP} \leq 0.63 \leq 10^5; \quad h = 120 \text{ mm} \quad [10]$$

Besides, the cavity flow *Cav* appeared under the cases of $d/d_b \leq 1$. $Cd_{TP}/(Cd_{SP})_{Sub}$ in these cases was the following value within errors ±6% except for the slightly low values under the condition of $d = 1$ mm and $\bar{\alpha}_0 \leq 0.05$.

$$(Cd_{TP})_{Cav}/(Cd_{SP})_{Sub} = 0.60$$

$$1 \text{ mm} \leq d \leq 6 \text{ mm}, 0 \leq \bar{\alpha}_0 \leq 0.1, 0.038 \times 10^5 \leq \text{Re}_{TP} \leq 0.38 \times 10^5 \quad [11]$$

Finally, with increasing of $\bar{\alpha}_0$ under any pair of conditions of d and Re_{TP}, the flow changed into the transcritical type in the two-phase flow *TPTrans* or the cavity flow *Cav* at last, i.e. it was concluded that the drag coefficient ratio $Cd_{TP}/(Cd_{SP})_{Sub}$ always changed to reach 0.6 as $\bar{\alpha}_0$ increased.

5. CONCLUSIONS

1. The flow pattern of the two-phase wake flow behind a cylinder changed from the subcritical type *Sub* or the supercritical one *Sup* in the single-phase flow to the new one *TPTrans* in the two-phase flow with increasing of the mean void fraction $\bar{\alpha}_0$, under various conditions of the cylinder diameter and the Reynolds number of the two-phase flow Re_{TP}. Under the condition of $\text{Re}_{TP} \leq 0.63 \times 10^5$, the transition from *Sub* to *TPTrans* occurred. On the other hand, the transition from *Sup* to *TPTrans* took place under the condition of $\text{Re}_{TP} \geq 1.3 \times 10^5$. $\bar{\alpha}_0$ at which the *Sub* → *TPTrans* transition terminated became small as d increased, though the *Sup* → *TPTrans* transition depended little on d.

The distribution of static pressure on the cylinder surface and the drag coefficient of *TPTrans* in the two-phase flow were truly similar to those of the transcritical type *Trans* in the single-phase flow. Therefore, assuming that *TPTrans* corresponds to *Trans*, it is concluded that the upper transition Reynolds number in the two-phase flow, at which the flow pattern changes to reach the transcritical type, is less than the lower transition Reynolds number in the single-phase flow.

In cases of $d/d_b \leq 1$, when $\bar{\alpha}_0$ increased, the sudden transition to the cavity flow appeared at a certain value of $\bar{\alpha}_0$. The smaller d became, the smaller the value got, so that the region where the cavity flow appeared enlarged with decreasing of d.

2. The drag coefficients in the two-phase flow are correlated by formulas [8] and [10] except for the near of the critical Reynolds number in the single-phase flow under which the change of the drag coefficient was complex. Although the trend of increase with $\bar{\alpha}_0$ could be

expressed by formula [8], it was considered that the drag coefficient ratio $Cd_{TP}/(Cd_{SP})_{Sub}$ approached 0.6 corresponding to *TPTrans* as $\bar{\alpha}_0$ increased further. Also in the near of the critical Reynolds number, Cd_{TP} approached to the curve of formula [8].

Besides, $Cd_{TP}/(Cd_{SP})_{Sub}$ of the cavity flow was about 0.6 without dependency on Re_{TP}.

Finally, it is concluded that the flow pattern of the two-phase flow changes to either the transcritical type in the two-phase flow or the cavity flow with increase of the mean void fraction in the main flow, and therefore, the drag coefficient ratio $Cd_{TP}/(Cd_{SP})_{Sub}$ always reaches 0.6 at last. Consequently, the possibility of reduction in the drag coefficient of a cylinder in a two-phase flow is confirmed.

Acknowledgements—This work has been performed by a part of the Grant-in-Aid for Scientific Research of the Ministry of Education, Science and Culture under Grant No. 342052. The authors would like to thank Mr. H. Matsuura and Mr. M. Sekiguchi (they were graduate students of the Tokyo Institute of Technology) for their assistance in conducting our experiments.

REFERENCES

DELANY, N. K. & SORENSEN, N. E. 1953 Low-speed drag of cylinders of various shapes. NACA TN 3038.

FUNG, Y. C. 1960 Fluctuating lift and drag acting on a cylinder in flow at super-critical Reynolds numbers. *J. Aero Space Sci.* **27**, 801–814.

PURSNALL, W. J. & LOFTIN, L. K. 1951 Experimental investigation of localized regions of laminar-boundary-layer separation. NACA TN 2338.

ROSHKO, A. 1954 On the drag and shedding frequency of bluff cylinders. NACA TN 3169.

ROSHKO, A. 1955 On the wake and drag of bluff bodies. *J. Aero Space Sci.* **22**, 124–132.

ROSHKO, A. 1961 Experiments on the flow past a circular cylinder at very high Reynolds number. *J. Fluid Mech.* **10**, 345–356.

SURRY, D. 1972 Some effects of intense turbulence on the aerodynamics of a circular cylinder at subcritical Reynolds number. *J. Fluid Mech.* **52**, 543–563.